Colloids and Surfaces B: Biointerfaces 126 (2015) 489–495

Contents lists available at ScienceDirect

Colloids and Surfaces B: Biointerfaces

journal homepage: www.elsevier.com/locate/colsurfb

Assessment of surfactants for efficient droplet PCR in mineral oil using the pendant drop technique

Kunal R. Pandit[a], Paul E. Rueger[a], Richard V. Calabrese[a], Srinivasa R. Raghavan[a,b], Ian M. White[b,*]

[a] Department of Chemical and Biomolecular Engineering, University of Maryland, College Park, MD 20742, United States
[b] Fischell Department of Bioengineering, University of Maryland, College Park, MD 20742, United States

ARTICLE INFO

Article history:
Received 25 August 2014
Received in revised form
11 December 2014
Accepted 4 January 2015
Available online 10 January 2015

Keywords:
Pendant drop
Droplet PCR
Brij

ABSTRACT

Amplification and detection of nucleic acid sequences within integrated microsystems is routinely conducted using the technique of droplet PCR, wherein the polymerase chain reaction (PCR) is performed in microscale water-in-oil droplets (nanoliter to picoliter volumes). During droplet PCR, interactions at the interface of the droplet tend to dominate. Specifically, adsorption of the polymerase at the droplet interface leads to inefficient amplification. To reduce polymerase adsorption, surfactants such as the silicone-based ABIL EM90 have been commonly used. However, these surfactants have been selected largely through trial and error, and have been only somewhat effective. For example, when using ABIL EM90, 8 times (8×) the manufacturer prescribed concentration of polymerase was necessary for amplification. In this report, we use the pendant drop technique to measure adsorption and loss of enzyme at droplet interfaces for various surfactant-oil combinations. Dynamic interfacial tension and surface pressure measurements showed that significant polymerase adsorption occurs when using ABIL EM90. In contrast, much lower polymerase adsorption is observed when using Brij L4, a nonionic surfactant with a C_{12} tail and an oxyethylene headgroup, which has not yet been reported for droplet PCR. These results correlate strongly with droplet PCR efficiency. Brij L4 enables highly efficient PCR at 2× polymerase concentration, and still enables effective PCR at 1× polymerase concentration. Overall, this work introduces a methodology for quantitatively assessing surfactants for use with droplet microreactors, and it demonstrates the practical value of this new approach by identifying a surfactant that can dramatically improve the efficiency of droplet PCR.

1. Introduction

Polymerase chain reaction (PCR) is a powerful biochemical technique to amplify, quantify, and identify specific genes related to cancers [1], infectious diseases [2], forensics [3,4], and hereditary disorders [5]. Bulk PCR, which is commonly performed in central lab environments, involves the thermal cycling of 20–50 μL of aqueous solutions in well plates. The process, including sample preparation, takes several hours and requires a number of manual steps. The duration of PCR from sample preparation to DNA analysis can be reduced by integrating laboratory functions in micro total analysis systems. An important and widely used element of these systems is the droplet PCR component. Ultrafast droplet PCR has been achieved with integrated heaters, where 40 thermal cycles have been conducted in under 6 min [6].

Droplet PCR uses microfluidic techniques to apportion PCR reaction mixtures into aqueous droplets ("microreactors") surrounded by an oil phase. Typically droplets are in the micrometer size range and their volumes range from nanoliters to picoliters. At the larger size range, DNA is quantified using a cycle threshold calibration curve. In comparison, for picoliter droplets, DNA is absolutely quantified using a popular variation of PCR termed digital PCR. The initial average DNA copy number per droplet in digital PCR is less than 1, implying a Poisson distribution with either 0 copies or 1 copy in most droplets [7]. After thermal cycling, only droplets containing the target DNA fluoresce. The number of fluorescent droplets is then counted to quantify the amount of target DNA via Poisson statistics. Digital PCR has been shown to quantify extremely rare targets, such as HIV DNA in infected patients undergoing effective treatment [2].

Though impactful, droplet PCR is in need of technical improvement. Microreactors less than microliters in volume are dominated

* Corresponding author. Tel.: +1 3014056230; fax: +1 301 405 9953.
E-mail address: ianwhite@umd.edu (I.M. White).

http://dx.doi.org/10.1016/j.colsurfb.2015.01.001
0927-7765/

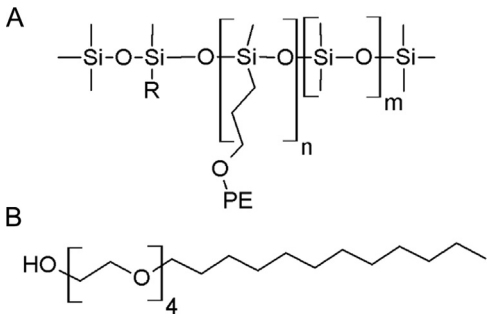

Fig. 1. Structure of the surfactants used in this study. (A) ABIL EM90, a silicone-based surfactant where R is an *n*-alkyl chain and PE is —$(CH_2)_3$—O—$(C_2H_4O)_x$—$(C_3H_6O)_y$—H. (B) Brij L4, a nonionic surfactant with a headgroup composed of 4 oxyethylene units and an *n*-dodecyl tail.

by surface effects [8]. The increase in surface area relative to the volume of the droplet is advantageous for rapid heat transfer. However, adsorption of proteins to the water–oil interfaces hinders droplet PCR. Specifically, Taq polymerase (Taq Pol), an enzyme derived from thermophilic bacteria, is used in PCR to catalyze the reaction. Taq Pol is a relatively hydrophobic enzyme and thus is especially prone to adsorption at interfaces. The aliphatic index characterizes the relative hydrophobic volume of a protein and, in general, thermophilic bacterial proteins have large relative hydrophobic volumes to aid in structural stability at high temperatures [9]. The aliphatic index of Taq Pol is 98.6; in comparison, the aliphatic index of bovine serum albumin (BSA), a protein commonly used in molecular biology techniques, is 76.1. Indeed, Taq Pol is incredibly stable; even at DNA melting temperatures of 95 °C, the half-life of Taq Pol is 45–50 min [10].

Several techniques have been reported in the literature to overcome Taq Pol adsorption in microfluidic droplets. One obvious method is to increase the Taq Pol concentration to replace adsorbed enzyme [8]. However, this is a wasteful approach and has been shown to require up to 7 times (7×) the Taq Pol needed for bulk PCR [11]. Another easy and popular method is to increase the amount of surfactant used in the system [12]. While surfactants are needed to stabilize the water droplets in oil, they can also competitively bind to the interface and thus reduce Taq Pol adsorption (although excessive surfactant can inhibit PCR). Similarly, inactive proteins like BSA may be included in the PCR mixture to competitively bind to the interface. Usually, both methods are employed simultaneously. For example, one protocol calls for the PCR aqueous phase to be supplemented with 0.5 g/L of BSA and the mineral oil phase with 2 vol% ABIL EM90 [13]. Alternatively, fluorinated oils and surfactants have been used with Taq Pol at room temperature to create droplets for digital PCR [5]. However, this requires fluorocarbon specialty chemicals, which increases costs and concerns for the environment. A system that relies on a cheap and widely available oil phase, such as mineral oil, would be preferred.

In this report, we focus on the use of surfactants to prevent the adsorption and loss of polymerase in droplet PCR. Previous studies with droplet PCR that have investigated the type and concentration of surfactant have mostly relied on trial and error. Here, we establish the use of the pendant drop technique for quantitative assessment and comparison of surfactants in droplet PCR [14,15]. In this technique, an aqueous drop is suspended in oil at the tip of a syringe. The geometry of the drop determines the interfacial tension. By performing the pendant drop test with an aqueous drop of Taq Pol suspended in mineral oil containing surfactant, we measure the adsorption of enzyme and/or surfactant at the droplet interface [16–18].

Thus, this simple test can assess the capability of a surfactant to inhibit the adsorption of Taq Pol. Among the surfactants, we have specifically examined ABIL EM90, a silicone-based surfactant (Fig. 1a) which is commonly used for droplet PCR [19]. Our studies show that ABIL EM90 is unable to prevent significant Taq Pol adsorption and loss. On the other hand, as an alternative, we have identified a simple, inexpensive surfactant, Brij L4 (Fig. 1b), which has an alkyl tail attached to an oxyethylene head group. Brij L4 ensures negligible adsorption of Taq Pol at the droplet interface. In turn, when PCR is conducted in picoliter droplets in the presence of Brij L4, fewer cycles and less Taq Pol are needed to reach the fluorescence threshold compared to the case of ABIL EM90. Brij L4 is thus a superior alternative for droplet PCR. To our knowledge, this is the first report of Brij L4 for this purpose.

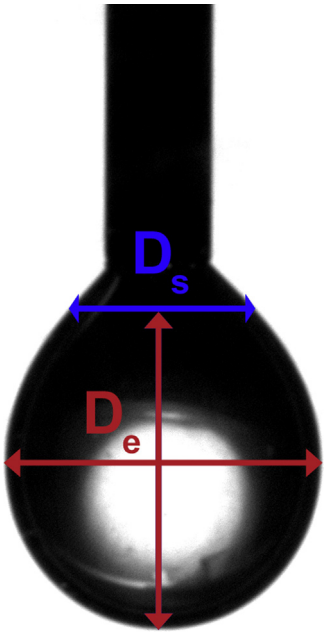

Fig. 2. Measurement of interfacial tension between water and oil from the shape of a pendant droplet. The photograph shows an aqueous droplet (diameter ~1–5 mm) hanging from a needle in a solution of mineral oil. Droplet width is measured at two points, as shown: the largest equatorial width D_e, and the width D_s at a distance of D_e from the tip. The interfacial tension is correlated with D_e and D_s using Eq. (1).

2. Materials and methods

2.1. Interfacial tension measurement

Interfacial tension measurements were taken using a dynamic pendant drop technique. An aqueous drop with an initially clean interface is formed in oil. As time proceeds, enzyme and/or surfactants adsorb at the interface, lowering the interfacial tension until the equilibrium interfacial tension is achieved. Transient drop shape factors were determined from images by measuring in millimeters the largest width of the drop D_e and the width of the drop D_s at a distance equal to D_e from the bottom of the drop (Fig. 2). These were empirically correlated to the interfacial tension γ in dynes per centimeter using Eq. (1), where g is the acceleration due to gravity in meters per second squared, and $\Delta\rho$ is the difference in density between the water and oil phases in kilograms per meter cubed [20].

$$\gamma = 3.17 g \Delta\rho D_e^{-0.08} D_s^{2.08} \quad (1)$$

Stock solutions of 1.5% (w/w) ABIL EM90 (Evonik Industries) and 0.5% (w/w) Brij L4 (Sigma–Aldrich) in mineral oil (light oil, BioReagent, suitable for mouse embryo cell culture, Sigma Aldrich) were stored at room temperature. The ABIL EM90 concentration was chosen based on previous studies [13]. The Brij L4 concentration

was the highest that allowed for sufficiently sized droplets that would not detach from the needle tip over an hour. Aqueous solutions of Taq Pol (BioRad) consisting of 20 mM Tris HCl, 50 mM KCl, and 1.5 mM $MgCl_2$ were made the day of experiments and stored on ice. The concentration of Taq Pol in the aqueous droplet phase ranged from 0 to 8×, where 1× was 0.025 U/μL (the concentration prescribed by the manufacturer for a 50 μL reaction).

Mineral oil solutions were preheated and maintained at 55 °C with a water bath during all experiments to obtain measurements at relevant elevated PCR temperatures (higher temperatures caused observable bubble formation in the water bath, which obscured the droplet). The density of mineral oil at 55 °C was measured to be 0.806 ± 0.005 g/mL. The density of the aqueous solutions was taken to be 0.986 g/mL, the density of water at 55 °C [21]. The viscosity of the light mineral oil at 55 °C was measured using an Advanced Rheometer 2000 thermally controlled cone-and-plate rheometer and found to be 9.2 mPa s.

Hanging aqueous droplets were formed in mineral oil solutions at the tip of either 16, 18, or 26 gauge syringe needles to form the largest non-spherical droplets that would not pinch off. No difference was seen in γ with different sized needles. Syringes were rinsed thoroughly with ultrapure deionized water and dried with nitrogen between experiments. Interfacial tensions for each time point were calculated from 5 images of the pendant droplet acquired using a Pulnix TM-1405GE CCD camera. The images were analyzed using ImageJ and Matlab software packages [22]. All equipment was setup on a vibration isolation table to minimize droplet movement, with the exception of the camera, which was stabilized on a tripod. The apparatus and experimental details are described elsewhere [22,23]. Each experimental condition was observed for at least 1 h and conducted in triplicate. The Bond number, defined as $Bo = \Delta\rho g D_e^2/\gamma$, was greater than 0.48 for all measured droplets, ensuring they were sufficiently non-spherical to allow for accurate measurements [24]. The maximum error in γ at each time point was 0.1 dyn/cm and the maximum error from drop to drop was 0.5 dyn/cm.

2.2. Real-time droplet PCR

To validate interfacial tension measurements, real-time PCR was performed, in which the change in fluorescence of individual PCR droplets was measured over each thermal cycle. The PCR master mix consisted of 20 mM Tris HCl, 50 mM KCl, 1.5 mM $MgCl_2$, 200 μM of each deoxynucleotide triphosphate (dNTP), 200 nM forward and reverse primers (forward primer: ACA GAG TTC TTG AAG TGG TGG; reverse primer: TGG TTT GTT TGC CGG GAT CAA), LC Green (Biofire Diagnostics), and varying concentrations of Taq Pol. The pUC19 (Thermo) plasmid served as the template for amplification. LC Green as supplied was diluted by a factor of 10 in the master mix. The initial concentration of pUC-19 was 5×10^6 copies/μL. Wells were fabricated by creating holes in 2.5 mm thick cured Sylgard 184 polydimethylsiloxane (PDMS, Dow Corning) using a 5 mm biopsy punch. Individual wells were separated and bonded to cover glass slips; bonding of the PDMS to glass was performed by spinning PDMS at 3000 rpm for 30 s on the glass to form a thin layer that served as an adhesive and as a hydrophobic bottom surface. Droplets, 20 ± 2 μm in diameter (~4 pL in volume) were formed in PDMS microfluidic chips using a 20 μm square channel flow focusing geometry (oil flow rate = 10 μL/min; aqueous flow rate = 2 μL/min) and then captured in wells filled with mineral oil solutions. Care was taken to capture single droplets in wells when using Brij L4 as the surfactant due to droplet coalescence during changes in temperature when thermal cycling. Wells were sealed with cover glass slips before thermal cycling on an aluminum plate heated and cooled with a Peltier.

Droplets were initially hot started at 95 °C for 3 min and then thermal cycled for 35 cycles. Each thermal cycle consisted of 30 s at 55 °C for annealing, 30 s at 72 °C for extension, and 30 s at 95 °C for melting. Real time amplification results were obtained after every extension step by exciting droplets using a blue LED (Innovations in Optics) with a Brightline 424–438 nm bandpass filter, while capturing fluorescence emission with a CCD (Allied Vision) fitted with a 67 mm working distance lens (Edmund Optics) and a high pass filter with a 475 nm cut-off (Omega Optical). The cycle threshold was defined as the cycle where the fluorescence during extension of a given cycle was greater than the fluorescence during the extension of the first cycle by 10 standard deviations. Data was taken from at least 3 droplets for each experimental condition.

2.3. Emulsion stability

Stable emulsions with Brij L4, a hydrophilic surfactant, were created by modifying the hydrophile–lipophile balance (HLB) with the addition of Span 80, a lipophilic surfactant. A ratio of 4:1 Span 80 to Brij L4 is required to form stable water in mineral oil emulsions at room temperature [25], though upon thermal cycling the emulsion broke. To find the optimal surfactant concentrations, emulsions with varying ratios of Span 80:Brij L4 in mineral oil were thermal cycled and then inspected under magnification to verify stability. A mixture of 5.0 wt% Span 80 and 0.5 wt% Brij L4 formed stable emulsions that withstood thermal cycles.

2.4. PCR for amplification factor determination

Emulsions of various mineral oil and surfactant mixtures with PCR master mix were thermal cycled to validate interfacial tension measurements with droplets in contact with one another. The PCR master mix consisted of 20 mM Tris HCl, 50 mM KCl, 1.5 mM $MgCl_2$, 200 μM of each dNTP, 200 nM forward and reverse primers (forward primer: GTC TCA TGA GCG GAT TAC A; reverse primer: CTC GTG ATA CGC CTA TTT TT), SYBR Green I (Lonza), and 1× or 2× Taq Pol. SYBR Green I as supplied was first diluted by a factor of 1000/3 in dimethylsulfoxide and then by a factor of 60 in the master mix. The pUC19 plasmid was again used as the template. The initial concentration of pUC-19 was 5×10^6 copies/μL. Mineral oil/surfactant mixtures used to create emulsions included 5.0% Span 80 & 0.5% Brij L4, 1.5% Span 80 & 0.5% Brij L4, and 1.5% ABIL EM90. PCR master mix was apportioned into droplets with the oil mixtures as the continuous phase as described in section 2.3. Droplets were directed into plastic conical PCR tubes where 20 μL of total droplet volume was collected in 10 min. Bulk PCRs were amplified by layering 100 μL of oil and surfactant mixtures on top of 20 μL of PCR master mix in plastic conical PCR tubes.

A MiniOpticon Real-Time PCR System (BioRad) was used to thermal cycle bulk and emulsion PCR reactions. The thermal cycles consisted of a 95 °C melt for 3 s followed by a 56 °C anneal for 30 s. The initial hot start was at 95 °C for 3 min followed by 20 cycles. Given a sufficient number of thermal cycles and active Taq Pol, the amount of DNA amplified during a PCR will plateau to a constant final amount of DNA regardless of the surfactant used. Thus to better differentiate effects of various oil/surfactant mixtures, the number of thermal cycles was chosen so that the amplification of DNA in bulk reactions would not reach the exponential phase. Each oil mixture and Taq Pol concentration was amplified in triplicate.

2.5. Oil extraction

The mineral oil/surfactant mixtures were separated from the aqueous phase using a liquid-liquid extraction technique adapted from Schaerli et al. [26]. First, emulsions were broken by centrifugation at 13,000 × *g* for 5 min and then excess upper oil phases were

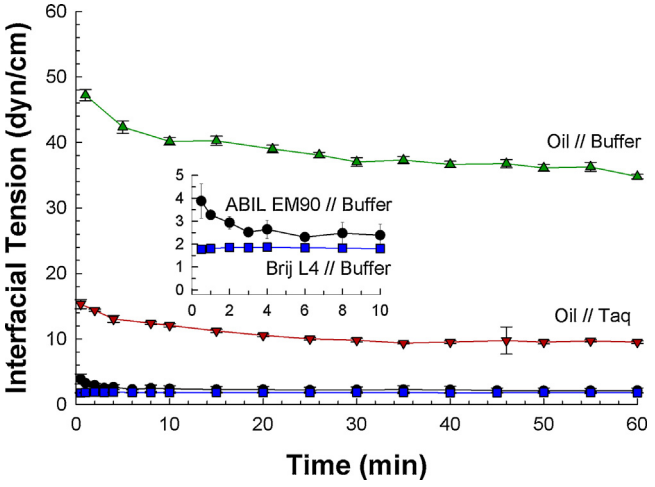

Fig. 3. Interfacial tension γ at the water–oil interface as a function of time t for various cases. At $t = 0$, the aqueous drop is suspended in mineral oil. The *green triangles* correspond to aqueous buffer (with no enzyme) in oil (with no surfactant). The *red triangles* represent the case where the Taq Pol enzyme is in the buffer (at a 1× concentration) and there is no surfactant in the oil. Finally, data are shown for two surfactants in the oil: 1.5 wt% of ABIL EM90 (*black circles*) and 0.5 wt% Brij L4 (*blue squares*); in each case the buffer contains no enzyme. The surfactants reduce γ and the equilibrium is reached rapidly, especially in the case of Brij L4. Points are averages of 3 trials. Error bars represent the standard deviation. (For interpretation of the references to color in this figure legend, the reader is referred to the web version of the article.)

removed. Next, the remaining oil was extracted twice by addition of 0.5 mL of water-saturated diethyl ether, sample vortexing, and upper organic phase disposal. Finally, the residual organic phase was evaporated in a fume hood at room temperature for 10 min.

2.6. Amplification factor measurement

The amount of DNA amplified after 20 thermal cycles was quantified using qPCR. The PCR reaction mixture consisted of iQ SYBR Green Supermix (BioRad) diluted by a factor of two, 200 nM forward and reverse primers (same as used in the amplification PCR), and the amplified DNA samples diluted by a factor of 10,000/3. The thermal cycle conditions were the same as the amplification PCR.

3. Results and discussion

3.1. Interfacial tension measurements for the study of Taq Pol adsorption

In our pendant drop experiments, we suspended an aqueous droplet in mineral oil at 55 °C (this temperature is relevant to an annealing step in a PCR thermal cycle). The interfacial tension of the water–oil interface γ was measured as a function of time. Typically, γ decreased with time, reaching an equilibrium within 45 min. Fig. 3 shows plots of $\gamma(t)$ for various cases.

In the absence of surfactants or enzyme, γ of the water–oil interface has a value of 36.4 dyn/cm at equilibrium (we denote this as γ_0). The decrease in γ over time was not surprising because of possible surface active contamination in the mineral oil. In any case, γ_0 was used as a reference point to determine further adsorption of surfactants or proteins. When either surfactant or enzyme is present, γ is much lower. Specifically, when 1× Taq Pol is present in the aqueous phase and there is no surfactant in the oil, γ is 15.3 dyn/cm at $t = 0$ and decreases to 9.6 dyn/cm at equilibrium. On the other hand, when the buffer with no Taq Pol is contacted with oil containing 1.5 wt% of the silicone surfactant ABIL EM90, γ is 3.8 dyn/cm at $t = 0$ and 2.2 dyn/cm at equilibrium (we denote the latter value as γ_{A0}). Lastly, when the buffer with no Taq Pol is contacted with oil containing 0.5 wt% of Brij L4, γ is at 1.82 dyn/cm, and is nearly constant with time (we denote this value as γ_{B0}).

The above dynamic measurements reflect the adsorption of enzyme and surfactant at the droplet interface. As soon as the droplet is formed, surfactant or enzyme molecules migrate to the interface, causing the interfacial tension γ to decrease relative to its value without surface active molecules (i.e., γ_0). For the case of Taq Pol alone (no surfactant), the decrease in γ from its initial to steady-state value occurs quite slowly (over about 30 min). This shows that Taq Pol adsorption at the interface continues well after droplet formation. In comparison, when using ABIL EM90 (in the oil), γ has a lower initial value and also reaches its equilibrium faster (in about 10 min). In this case, the interface will initially have adsorbed surfactant, but it is evidently not saturated. The decrease in γ with time likely reflects additional adsorption of surfactant from the oil. Lastly, when using Brij L4 (in the oil), we note that γ reaches an equilibrium very quickly (in <2 min), implying that the interface is rapidly saturated with surfactant molecules.

The initial interfacial tension γ of surfactant or protein systems was very low compared to γ_0, thus the interface was under a high surface pressure $\Pi = \gamma_0 - \gamma$. Adsorption to a high Π film is limited by penetration to the interface, where there is a considerable surface excess concentration of amphiphiles. The kinetics of adsorption at liquid–liquid interfaces in the presence of excess amphiphile is usually interpreted in terms of the model of Ward and Tordai [27]. According to this model, for the case of adsorption limited kinetics, the variation of the surface pressure Π with time is given by Eq. (2):

$$\frac{d\Pi}{dt} = k_f \nu \cdot C \cdot \exp\left(-\frac{\Pi \Delta A}{k_B T}\right) \tag{2}$$

where k_f is the adsorption rate constant, ν is the number of adsorbing groups, C is the bulk concentration of the amphiphile, ΔA is the area created in the interfacial film to adsorb the species, and $\Pi \Delta A$ is the work to create the area ΔA in a film under surface pressure Π. The above equation assumes that the adsorption of the amphiphile is irreversible and it can be rewritten in the following form:

$$\ln\left(\frac{d\Pi}{dt}\right) = \ln(k_f \nu \cdot C) - \frac{\Pi \Delta A}{k_B T} \tag{3}$$

Fig. 4 shows a plot of $\ln(d\Pi/dt)$ as a function of Π for the case of 1× Taq Pol in the aqueous droplet and no surfactant in the oil. The initial linear portion of the plot at low surface pressures is fitted to Eq. (3) using a linear least squares fit. The slope of the line is proportional to ΔA, which is the area occupied by a Taq Pol molecule on the interface [14]. We calculate $\Delta A = 4 \pm 1$ nm^2. For comparison, $\Delta A = 2$ nm^2 for BSA, a much smaller protein. The significance of this parameter is that if a space in the interfacial film of 4 nm^2 is cleared, Taq Pol would still be able to migrate from solution and adsorb at the interface.

Previously, Angione, et al., estimated adsorption of Taq Pol based on diffusion limited adsorption theory and correlating production of DNA to Taq Pol concentrations in bulk reactions [8]. Our results indicate that the protein film is under a high surface pressure Π, and therefore is not diffusion limited but kinetically limited. Furthermore, Angione, et al., determined that the area per molecule of Taq Pol at the water–oil interface reasonably agreed with an estimate of the radius of gyration of the polymerase in a denatured conformation (116 Å). However our interfacial tension data suggests that Taq Pol could further adsorb between gaps in the film that are smaller than the enzyme in size (native radius of gyration = 38.3 Å). This minimal area required for adsorption is likely due to the enzyme's large hydrophobic content. Only a small hydrophobic portion of Taq Pol is necessary to interact with the interface for the enzyme to irreversibly adsorb.

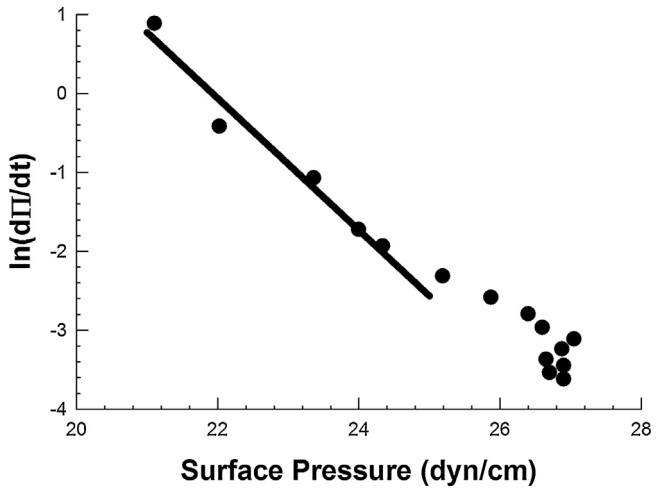

Fig. 4. Dynamics of Taq Pol adsorption to the water–oil interface in the absence of surfactant. The $\gamma(t)$ from Fig. 2 (*red triangles*) is replotted in terms of the surface pressure $\Pi = \gamma_0 - \gamma$, where γ_0 is the interfacial tension at steady state of a bare interface. The plot above is a semilog plot of $d\Pi/dt$ vs. $\Pi(t)$, as suggested by Eq. (3). A straight line fit to the initial linear region at low Π yields the value of ΔA, which is the area occupied by Taq Pol at the interface.

Next, we proceeded to measure the interfacial tension γ vs. time for different concentrations of Taq Pol in the aqueous phase and 1.5 wt% ABIL EM90 in the oil phase. Fig. 5a plots $(\gamma_{A0}-\gamma)$ for representative polymerase concentrations (data at other concentrations is shown in the Supplementary data, Fig. S1). Note that γ_{A0} is the equilibrium interfacial tension for mineral oil with 1.5 wt% ABIL EM90 in contact with aqueous buffer (as measured in Fig. 3). At low Taq Pol (0.1×) and moderate Taq Pol (1.4×), $\gamma(t)$ shows a monotonic behavior, and equilibrium is reached within 20 min. When the polymerase concentration was greater than or equal to 2×, a non-monotonic trend was seen, as indicated in Fig. 5a for the case of 8× Taq Pol. Here, the function initially shows an overshoot from its initial value before decreasing to a steady-state within about 20 min. The overshoot is likely due to the displacement of surfactant molecules from the interface by protein.

Similarly, we measured the interfacial tension γ vs. time for various concentrations of Taq Pol in the aqueous phase and 0.5 wt% Brij L4 in the oil phase. Plots of $(\gamma_{B0}-\gamma)$ for representative protein concentrations are shown in Fig. 5b (data at other concentrations is shown in the Supplementary data, Fig. S2). Note that γ_{B0} is the steady-state interfacial tension for mineral oil with 0.5 wt% Brij L4 in contact with buffer (as measured in Fig. 3). The plots are all nearly flat, i.e., the interfacial tension is nearly constant over time at all polymerase concentrations. This suggests that the interface is rapidly saturated with Brij L4 and that the Taq Pol does not displace the surfactant from the interface. In other words, Brij L4 is able to prevent the adsorption of polymerase over the course of our experiments.

The surface pressure Π_S at equilibrium as a function of Taq Pol concentration is shown in Fig. 6 for both surfactants (i.e., these are the equilibrium data from Figs. 5, S1, and S2). When 1.5% of ABIL EM90 is in the oil, Π_S increases with polymerase concentration before leveling out. This indicates that both Taq Pol and ABIL EM90 adsorb at the interface. It is only when 4× Taq Pol is in solution that the interface is fully saturated at $\Pi_S = 35.2$ dyn/cm. These results are in sharp contrast to the case when 0.5% Brij L4 is present in the oil; Π_S is constant at 3.6 dyn/cm over all polymerase concentrations. In other words, Brij L4 rapidly saturates the water–oil interface and thus prevents significant adsorption of the enzyme. These results suggest that Brij L4 is likely to be a better surfactant for droplet PCR than ABIL EM90. It should be noted that the

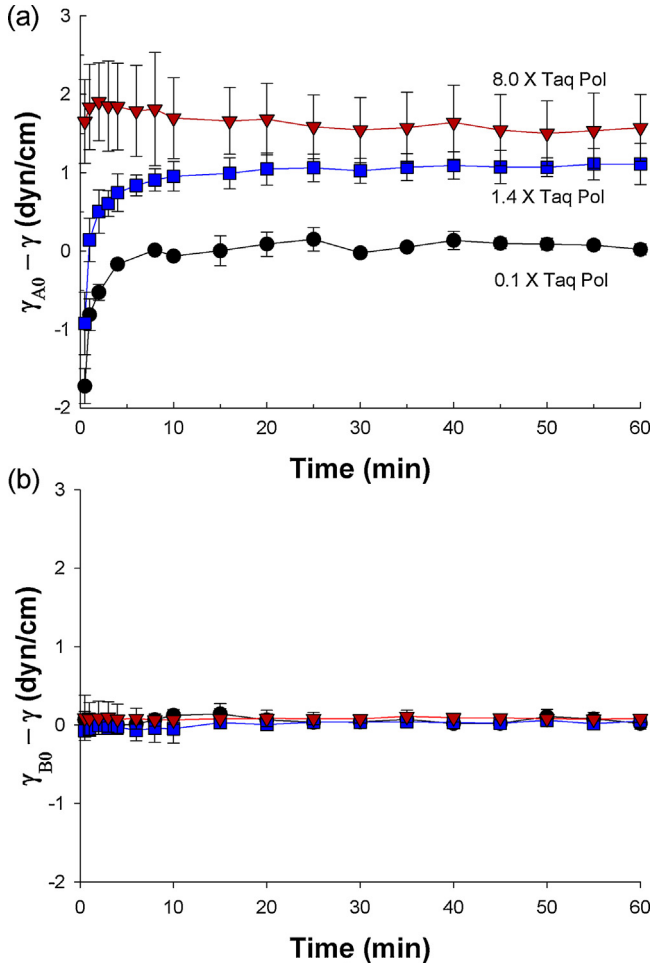

Fig. 5. Interfacial tension as a function of time t with surfactant in the oil phase and protein in the aqueous phase. (a) 1.5 wt% ABIL EM90 in the oil phase and various concentrations of Taq Pol in the aqueous phase. The data is plotted as the deviation from the steady state interfacial tension γ_{A0} for mineral oil with 1.5 wt% ABIL EM90 in contact with buffer (from Fig. 3). In all cases, a steady state is reached within about 20 min. (b) 0.5 wt% Brij L4 in the oil phase and various concentrations (same as in (a)) for Taq Pol in the aqueous phase. In this case the data is plotted as the deviation from the steady state interfacial tension γ_{B0} for mineral oil with 0.5 wt% Brij L4 in contact with buffer (from Fig. 3). The steady state is reached immediately in all cases.

droplet size in the pendant drop measurements is in the millimeter range (volumes in the microliters). If the droplets are instead in the microscale range of diameters (picoliter volumes), the surface-to-volume ratios would be even higher and therefore even at 4× Taq Pol, much of the enzyme could be adsorbed at the interface and thereby rendered non-functional.

3.2. Real-time droplet PCR validation

To examine whether Brij L4 is indeed a superior surfactant for PCR, we performed droplet PCR with droplets of 20 μm diameter (~4 pL volume). Aqueous droplets containing the pUC-19 plasmid, Taq Pol, and the rest of the components of the PCR master mix were captured in wells filled with mineral oil containing dissolved surfactant (ABIL EM90 or Brij L4). At this droplet size, the number of initial copies of pUC-19 per droplet varies probabilistically with an average of 20 initial plasmids. Droplets were thermal cycled (as described above), and fluorescence from the droplets was measured in real-time. When the PCR was successful, all observed droplets amplified. In each cycle of PCR, primers hybridize to template DNA to form a partially double stranded segment and

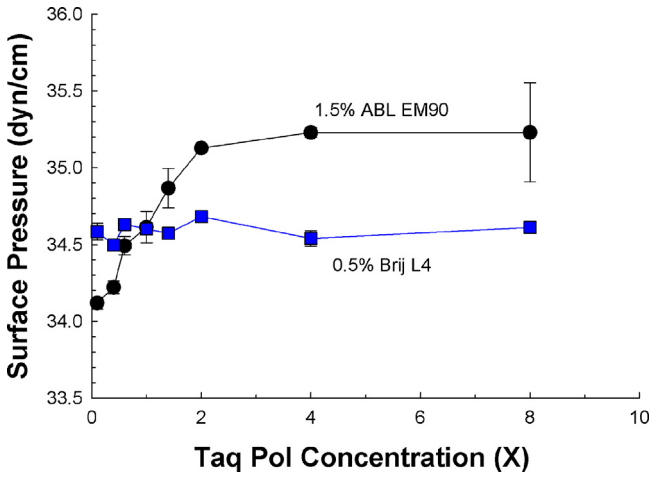

Fig. 6. Influence of surfactants on Taq Pol adsorption, measured for different polymerase concentrations. The surface pressure Π_S at equilibrium is shown as a function of polymerase concentration (denoted by the multiple ×, where 1× is 0.025 U/μL) for the two different surfactants, 1.5 wt% ABIL EM90 (*black*) and 0.5 wt% Brij L4 (*blue*). In the case of ABIL EM90, Π_S increases with Taq Pol, indicating that both the surfactant and the enzyme adsorb at the interface. In the case of Brij L4, Π_S is independent of Taq Pol, indicating that the surfactant saturates the interface, thereby minimizing adsorption of the enzyme. (For interpretation of the references to color in this figure legend, the reader is referred to the web version of the article.)

are subsequently extended by Taq Pol. If the PCR is efficient, all bound primers are extended every cycle and the copies of amplicons roughly double over each cycle. This is achieved if sufficient active polymerase is in solution to catalyze the extension of bound primers. An excess of Taq Pol would have no effect on the cycle threshold, whereas a depletion of Taq Pol would decrease the cycle efficiency of PCR and thus increase the cycle threshold.

Fig. 7 shows the cycle threshold for droplet PCR as a function of Taq Pol for the two surfactants under study (real-time data is presented in the Supplementary Material in Fig. S3). The results confirm that the PCR cycle efficiency is significantly better when 0.5 wt% Brij L4 is used than when 1.5 wt% ABIL EM90 is used. Using

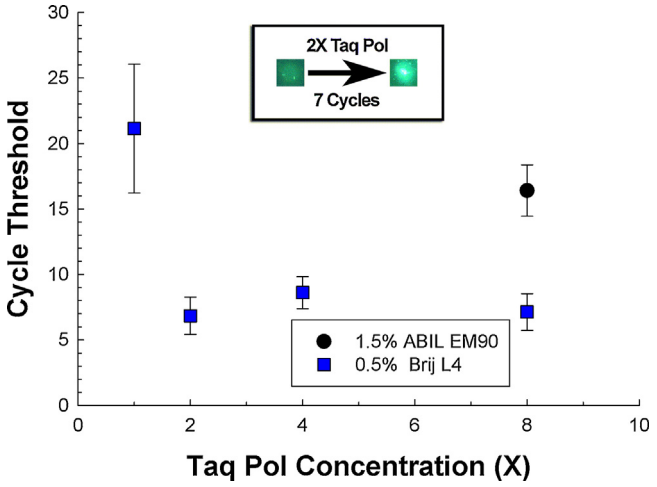

Fig. 7. Cycle threshold during droplet PCR for various Taq Pol concentrations and in the presence of surfactant. The data show that efficient PCR can be accomplished when 0.5% Brij L4 (*blue*) is used in the oil phase. For Taq Pol concentrations from as little as 2× to 8×, only ~7 cycles are necessary to reach the threshold. In comparison, with 1.5 wt% ABIL EM90 as the surfactant (*black*), PCR could not be performed with less than 8× Taq Pol, and even for that case, more cycles (~16) were needed. The inset shows raw images of a 20 μm diameter droplet revealing the increase in fluorescence from the initial cycle to the 7th cycle using 2× Taq Pol and 0.5% Brij L4. (For interpretation of the references to color in this figure legend, the reader is referred to the web version of the article.)

1.5% ABIL EM90 and 8× Taq Pol, 16 ± 2 cycles are necessary to reach the fluorescence threshold. In contrast, with 0.5% Brij L4, and at the same polymerase concentration, only 7 ± 1.5 cycles are required to reach the same threshold. Furthermore, PCR with ABIL EM90 could not be conducted to an appreciable level using less than 8× Taq Pol. On the contrary, when Brij L4 is present, efficient PCR was achieved with polymerase concentrations as low as 2×, with the threshold in this case being 7 ± 1.5 cycles as well. Even with 1× Taq Pol and with Brij L4, PCR could be performed, but 21 ± 5 cycles were necessary to reach the fluorescence threshold. Thus, when the enzyme concentration is very low, a fraction of it may still be lost due to competitive adsorption, though a significant amount of Taq Pol was still in solution that allowed for successful PCR. However, it is sufficient to use 2× Taq Pol to completely overcome any such losses due to adsorption.

Overall, we can conclude that using 0.5% Brij L4 significantly eliminates Taq Pol adsorption, as predicted by the pendant droplet and as validated by droplet PCR, as Brij L4 allows a 4-fold reduction (from 8× to 2×) in the Taq Pol necessary for efficient PCR. Furthermore, with 2× Taq Pol, the use of Brij L4 enables the fluorescence threshold to be reached in about half as many thermal cycles as compared to ABIL EM90 with 8× Taq Pol. Finally, successful PCR with Brij L4 also confirms that surfactant was not appreciably degraded during thermal cycling.

3.3. Emulsion PCR amplification factor validation

The above work demonstrated that Brij L4 was highly effective at preventing Taq Pol adsorption at the droplet interface, it was noted that care was required to prevent coalescence when using Brij L4. While many microfluidic droplet systems maintain control over the droplets such that coalescence is not an issue [28], some droplet PCR systems, including emulsion PCR, are subject to coalescence. We found that stable water-in-mineral-oil emulsions at PCR temperatures with 0.5% Brij L4 required the addition of 5.0% Span 80 to achieve stability. We compared this oil and surfactant mixture with 1.5% ABIL EM90, 1.5% Span 80 & 0.5% Brij L4, and bulk PCR by measuring the amplification factor after 20 thermal cycles using 1× Taq Pol in the aqueous phase (Fig. 8). Amplification factors of bulk PCRs were measured to be independent of the upper phase oil mixtures. An emulsion with 5% Span 80 in addition to 0.5% Brij L4 amplified about 3 orders of magnitude more DNA than bulk PCR. The droplet amplification was much more efficient due to the presence of nonionic surfactants, which stabilize and stimulate polymerase activity [29]. However, this increase in efficiency would only be possible with significant enzyme in solution. On the other hand the emulsion with 1.5% ABIL EM90 amplified about as much DNA as the bulk reaction. The 1.5% Span 80 and 0.5% Brij L4 emulsions broke whilst thermal cycling, thus amplification factors similar to bulk PCR were recorded.

Although 1.5% ABIL EM90 amplified about as much DNA as bulk PCR, our interfacial tension measurements and real-time droplet PCR results indicated that the amplification factor should be much less than bulk conditions. After we verified that the emulsion did not break during thermal cycling, we investigated the matter further by thermal cycling the emulsion for 35 cycles and comparing it to a bulk reaction. The amplification factor of the emulsion and bulk reactions after 35 cycles was 500 and $10^{5.6}$ respectively. Thus the 1.5% ABIL EM90 emulsion PCR was severely inhibited by a lack of functional Taq Pol in solution as suggested by our results in the previous sections. The lack of active Taq Pol was balanced with the increase in activity by a nonionic surfactant, which enabled the amplification factor at 20 cycles of the emulsion to be similar to the bulk.

The exponential increase in pUC19 product after 20 cycles using 5% Span 80 & 0.5% Brij L4 with as little as 1× Taq Pol indicated

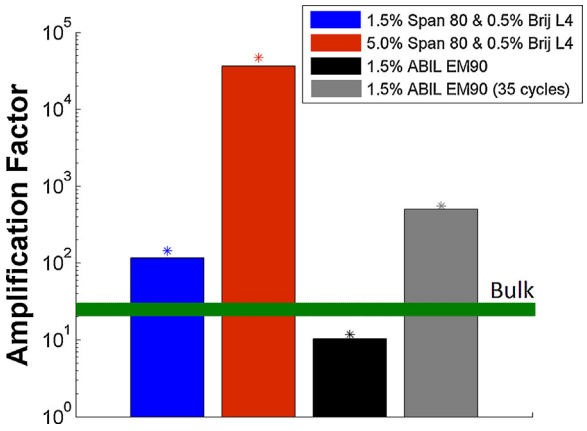

Fig. 8. Amplification factor of various emulsion PCRs with 1× Taq Pol. Amplification factor = copies of pUC19 product amplified after 20 thermal cycles/initial copies of pUC19. The *green line* provides a bulk PCR reference, which was independent of the different overlaid oil/surfactant mixtures. The 1.5% Span 80 & 0.5% Brij L4 emulsion (*blue bar*) was stable at room temperature but broke upon thermal cycling. Therefore, the amplification factor was similar to bulk PCR. The 1.5% ABIL EM90 emulsion (*black bar*), also had amplification factors similar to bulk PCR. When the PCR was extended to 35 cycles with 1.5% ABIL EM90 (*gray bar*), the amplification factor increased. However, the amount of DNA amplified was 3 orders of magnitude less than the bulk at 35 cycles. Amplification factors of 5.0% Span 80 & 0.5% Brij L4 (*red bars*), were about 3 orders of magnitude greater than that of bulk PCR. (For interpretation of the references to color in this figure legend, the reader is referred to the web version of the article.)

that a sufficiently large amount of active Taq Pol is blocked from the water–oil interface. However, our real-time droplet PCR results indicated 1× Taq Pol inefficiently amplified DNA. This discrepancy was probably due to more optimal thermal cycles in the emulsion PCR, which was performed in a PCR plate on a commercial thermal cycler instead of a custom-made system for microdevices. Furthermore, we believe the superior performance of this oil/surfactant mixture was attributed to the immediate saturation of the oil–water interface mostly by Brij L4 rather than Span 80. Without Brij L4, the 5 wt% Span 80 mineral oil emulsion broke during thermal cycling. The addition of a small amount of Brij L4, which stabilizes the droplet, suggested a large fraction of the interface was made up of Brij L4 to balance the Span 80. Additionally, although a large amount of Span 80 was required, it is a lipophilic surfactant. Thus much of the surfactant likely formed micelles in the oil phase which would slow adsorption of the Span 80 to oil–water interfaces [30].

In summary, the stable PCR emulsion with Brij L4 amplified orders of magnitude more DNA than the ABIL EM90 emulsion using only 1× Taq Pol. This is consistent with the surface tension measurements in Section 3.1 and validates the droplet PCR results of Section 3.2. Furthermore, this demonstration proved that droplet PCR with standard Taq Pol concentration is feasible with mineral oil, as opposed to fluorinated oils and surfactants, as done commercially today.

4. Conclusions

We have shown that the commercially available nonionic surfactant Brij L4 greatly enhances the efficiency of droplet PCR compared to a surfactant that is commonly used for this purpose, ABIL EM90. The superior effectiveness of Brij L4 is demonstrated by measurements of the water–oil interfacial tension using the pendant drop technique. When 0.5% Brij L4 is present in the oil, it rapidly migrates to and saturates the water–oil interface, in turn greatly inhibiting the adsorption of the Taq Pol enzyme from the water droplet to the same interface. In comparison, ABIL EM90 competes with the Taq Pol for the interface, and considerable enzyme is thus lost due to interfacial adsorption. These differences predict the performance of the surfactants in PCR experiments with picoliter droplets. Efficient DNA amplification is achieved in droplets coated with Brij L4 using standard concentrations of Taq Pol (as little as 1× or 2× Taq Pol relative to its standard concentration for bulk PCR). In contrast, 8× Taq Pol is needed to reach the cycle threshold in the case of ABIL EM90, and the threshold cycle number was significantly higher than that of Brij L4 with 2× Taq (16 vs. 7). Furthermore, stable Brij L4 emulsions akin to digital PCR methods were demonstrated and amplified 3 orders of magnitude more DNA than ABIL EM90 emulsions using standard concentrations of Taq Pol. Given that the cost of polymerase is ~10^6 times that of Brij L4, a reduction in Taq Pol by a factor of 4 or more corresponds to at least an 80% reduction in material costs.

Acknowledgments

This work was funded by Canon U.S. Life Sciences. The authors would also like to thank Dr. Alex Blake and Dr. Keith Herold for the use of their flatbed thermocycler system.

Appendix A. Supplementary data

Supplementary data associated with this article can be found, in the online version, at http://dx.doi.org/10.1016/j.colsurfb.2015.01.001.

References

[1] F. Moltzahn, A.B. Olshen, L. Baehner, A. Peek, L. Fong, H. Stöppler, J. Simko, J.F. Hilton, P. Carroll, R. Blelloch, Cancer Res. 71 (2011) 550.
[2] M.C. Strain, S.M. Lada, T. Luong, S.E. Rought, S. Gianella, V.H. Terry, C.A. Spina, C.H. Woelk, D.D. Richman, PLOS ONE 8 (2013) e55943.
[3] P. Liu, X. Li, S.A. Greenspoon, J.R. Scherer, R.A. Mathies, Lab Chip 11 (2011) 1041.
[4] J.A. Lounsbury, A. Karlsson, D.C. Miranian, S.M. Cronk, D.A. Nelson, J. Li, D.M. Haverstick, P. Kinnon, D.J. Saul, J.P. Landers, Lab Chip 13 (2013) 1384.
[5] D. Pekin, Y. Skhiri, J.-C. Baret, D. Le Corre, L. Mazutis, C. Ben Salem, F. Millot, A. El Harrak, J.B. Hutchison, J.W. Larson, D.R. Link, P. Laurent-Puig, A.D. Griffiths, V. Taly, Lab Chip 11 (2011) 2156.
[6] P. Neuzil, C. Zhang, J. Pipper, S. Oh, L. Zhuo, Nucleic Acids Res. 34 (2006) e77.
[7] N.R. Beer, B.J. Hindson, E.K. Wheeler, S.B. Hall, K.A. Rose, I.M. Kennedy, B.W. Colston, Anal. Chem. 79 (2007) 8471.
[8] S.L. Angione, A. Chauhan, A. Tripathi, Anal. Chem. 84 (2012) 2654.
[9] A. Ikai, J. Biochem. 88 (1980) 1895.
[10] F.C. Lawyer, S. Stoffel, R.K. Saiki, S.Y. Chang, P.A. Landre, R.D. Abramson, D.H. Gelfand, Genome Res. 2 (1993) 275.
[11] F. Wang, M.A. Burns, Biomed. Microdevices 11 (2009) 1071.
[12] A.C. Hatch, J.S. Fisher, A.R. Tovar, A.T. Hsieh, R. Lin, S.L. Pentoney, D.L. Yang, A.P. Lee, Lab Chip 11 (2011) 3838.
[13] R. Williams, S.G. Peisajovich, O.J. Miller, S. Magdassi, D.S. Tawfik, A.D. Griffiths, Nat. Methods 3 (2006) 545.
[14] E. Tornberg, J. Colloid Interface Sci. 64 (1978) 391.
[15] C.J. Beverung, C.J. Radke, H.W. Blanch, Biophys. Chem. 81 (1999) 59.
[16] R. Miller, V.B. Fainerman, A.V. Makievski, J. Krägel, D.O. Grigoriev, V.N. Kazakov, O.V. Sinyachenko, Adv. Colloid Interface Sci. 86 (2000) 39.
[17] R. Miller, V. Fainerman, A. Makievski, J. Krägel, R. Wüstneck, Colloids Surf. A: Physicochem. Eng. Asp. 161 (2000) 151.
[18] J.R. Lu, Annu. Rep. Sect. C: Phys. Chem. 98 (2002) 3.
[19] J.-C. Baret, Lab Chip 12 (n.d.) 422.
[20] A.W. Adamson, Physical Chemistry of Surfaces, 3rd ed., Wiley, New York, 1976.
[21] E.W. Lemmon, M.O. McLinden, D.G. Friend, NIST Stand. Ref. Database Number 69, National Institute of Standards and Technology, Gaithersburg, MD, 2012.
[22] P.E. Rueger, R.V. Calabrese, Chem. Eng. Res. Des. 05 (n.d.).
[23] P.E. Rueger, Liquid–Liquid Dispersions in Batch and In-Line Rotor Stator Mixers, University of Maryland, College Park, MD, USA, 2013.
[24] N.J. Alvarez, L.M. Walker, S.L. Anna, J. Colloid Interface Sci. 333 (2009) 557.
[25] The HLB SYSTEM: A Time-Saving Guide to Emulsifier Selection, ICI Americas Inc., Wilmington, DE, 1980.
[26] Y. Schaerli, R.C. Wootton, T. Robinson, V. Stein, C. Dunsby, M.A.A. Neil, P.M.W. French, A.J. Demello, C. Abell, F. Hollfelder, Anal. Chem. 81 (2009) 302.
[27] A.F.H. Ward, L. Tordai, Recl. Trav. Chim. Pay-Bas 71 (1952) 572.
[28] J.A. Kim, J.Y. Lee, S. Seong, S.H. Cha, S.H. Lee, J.J. Kim, T.H. Park, Biochem. Eng. J. 29 (2006) 91.
[29] H.-M. Eun, Enzymology Primer for Recombinant DNA Technology, Academic Press, Inc., San Diego, CA, 1996.
[30] X. Wang, Characterization of Surfactant Adsorption at a Liquid–Liquid Interface by Drop Volume Tensiometry. Masters thesis, Concordia University, 1997.

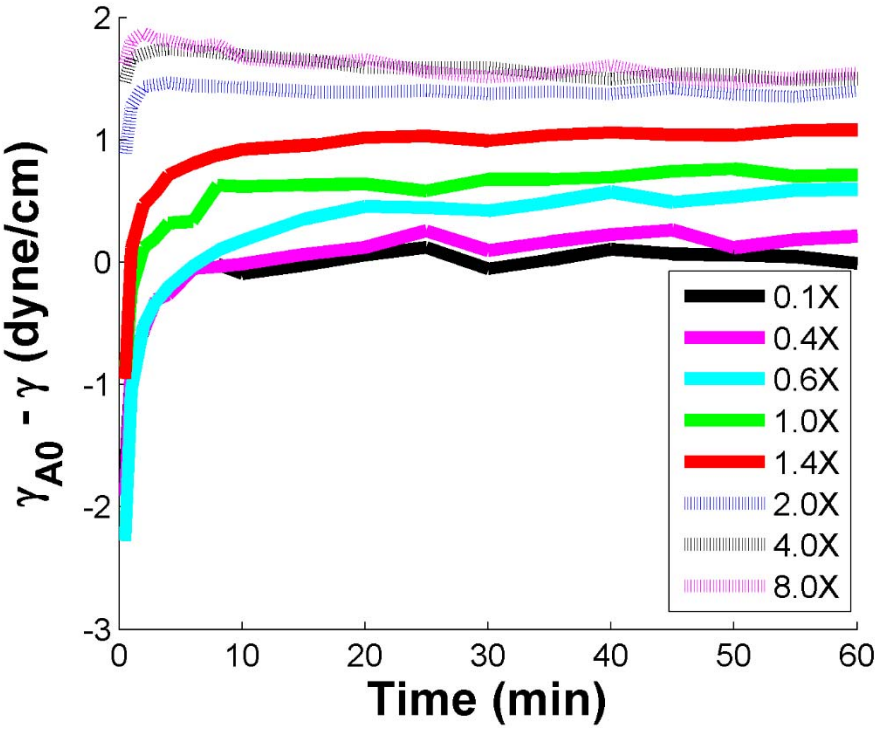

Figure S1. Interfacial tension as a function of time with 1.5 wt% ABIL EM90 in the oil phase and increasing Taq Pol concentration in the aqueous phase. The interfacial tension is plotted as the deviation from the equilibrium interfacial tension between buffer and an oil phase with 1.5 wt% ABIL EM90, ($\gamma_{A0} - \gamma$).

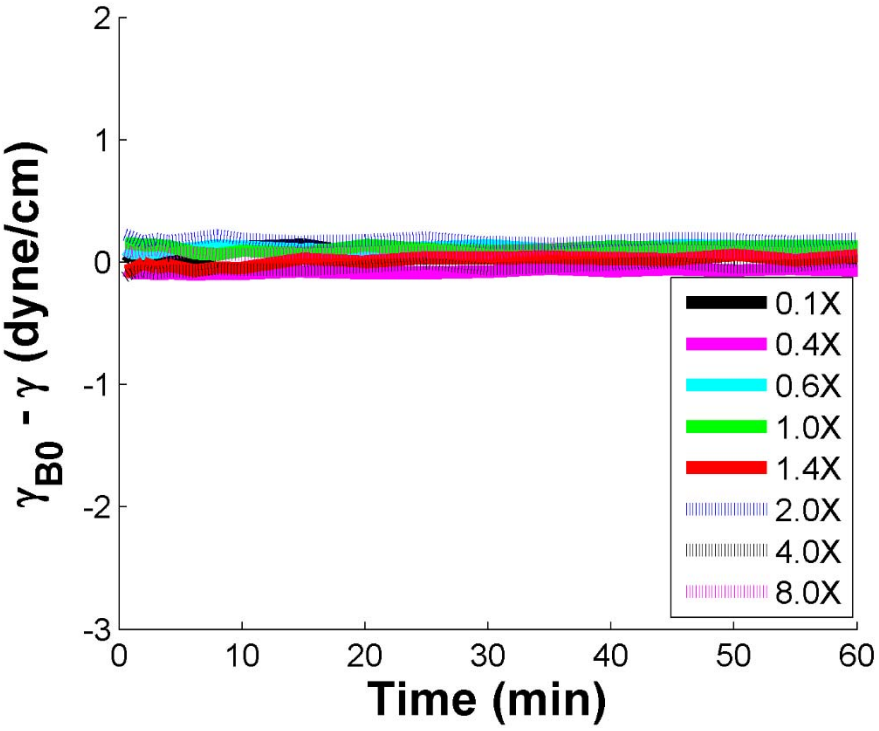

Figure S2. Interfacial tension as a function of time with 0.5 wt% Brij L4 in the oil phase and increasing Taq Pol concentration in the aqueous phase. The interfacial tension is plotted as the deviation from the equilibrium interfacial tension between buffer and an oil phase with 0.5 wt% Brij L4, ($\gamma_{B0} - \gamma$).

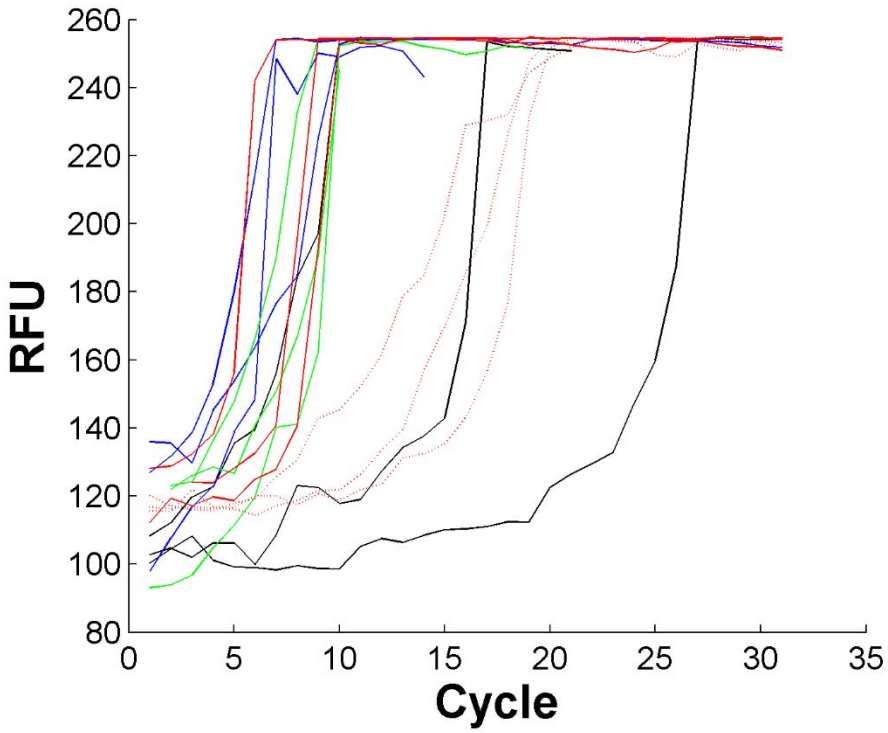

Figure S3. Raw fluorescence of droplets imaged during the extension step (72 ˚C) of a thermal cycle. The cycle threshold was determined as the cycle where the fluorescence was 10 times the standard deviation of the initial cycle. Amplification curves of 0.5 % Brij L4 (*solid lines*) and 1x (*black*), 2X (*blue*), 4X (*green*), and 8X (*red*) Taq Pol are shown. Droplets with 1.5 % ABIL EM90 only amplified with 8X Taq Pol (*dotted red*).